

Bending the Helicoid

William H. Meeks III* Matthias Weber†

July 6, 2018

Abstract

We construct Colding-Minicozzi limit minimal laminations in open domains in \mathbb{R}^3 with the singular set of C^1 -convergence being any properly embedded $C^{1,1}$ -curve. By Meeks' $C^{1,1}$ -regularity theorem, the singular set of convergence of a Colding-Minicozzi limit minimal lamination \mathcal{L} is a locally finite collection $S(\mathcal{L})$ of $C^{1,1}$ -curves that are orthogonal to the leaves of the lamination. Thus, our existence theorem gives a complete answer as to which curves appear as the singular set of a Colding-Minicozzi limit minimal lamination.

In the case the curve is the unit circle $\mathbb{S}^1(1)$ in the (x_1, x_2) -plane, the classical Björling theorem produces an infinite sequence of complete minimal annuli H_n of finite total curvature which contain the circle. The complete minimal surfaces H_n contain embedded compact minimal annuli \overline{H}_n in closed compact neighborhoods N_n of the circle that converge as $n \rightarrow \infty$ to $\mathbb{R}^3 - x_3$ -axis. In this case, we prove that the \overline{H}_n converge on compact sets to the foliation of $\mathbb{R}^3 - x_3$ -axis by vertical half planes with boundary the x_3 -axis and with $\mathbb{S}^1(1)$ as the singular set of C^1 -convergence. The \overline{H}_n have the appearance of highly spinning helicoids with the circle as their axis and are named *bent helicoids*.

Mathematics Subject Classification: Primary 53A10, Secondary 49Q05, 53C42

Key words and phrases: Minimal surface, curvature estimates, finite total curvature, minimal lamination, Björling's Theorem, bent helicoids, locally simply connected.

1 Introduction.

In [1], Colding and Minicozzi consider the question of the compactness of a sequence $\{M_n\}_{n \in \mathbb{N}}$ of embedded minimal surfaces in a Riemannian three-manifold N which are *locally simply connected* in the following sense: for each small open geodesic ball in N and

*This material is based upon work for the NSF under Award No. DMS - 0405836.

†This material is based upon work for the NSF under Award No. DMS - 0139476 and DMS - 0505557. Any opinions, findings, and conclusions or recommendations expressed in this publication are those of the authors and do not necessarily reflect the views of the NSF

for each n sufficiently large, M_n intersects the ball in disk components, with each disk component having its boundary in the boundary of the ball. They prove that every such sequence of minimal surfaces has a subsequence which converges to a possibly singular limit minimal lamination \mathcal{L} of N . In certain cases, the minimal lamination \mathcal{L} is nonsingular and is a minimal foliation of N . In this case, they prove that the singular set of C^1 -convergence consists of a properly embedded locally finite collection $S(\mathcal{L})$ of Lipschitz curves that intersect the leaves of \mathcal{L} transversely; we call such a limit foliation \mathcal{L} a *Colding-Minicozzi limit minimal lamination*.

In [13], Meeks and Rosenberg applied these results of Colding-Minicozzi to prove that the plane and the helicoid are the only properly embedded simply connected minimal surfaces in \mathbb{R}^3 . A standard blow-up argument then shows that small neighborhoods of points of large almost-maximal curvature on an embedded minimal surface of positive injectivity radius in a homogeneously regular three-manifold N have the appearance of homothetically shrunk helicoids. An application by Meeks [6, 5] of this local picture for a minimal disk centered at a point of large almost-maximal curvature demonstrates that the singular curves $S(\mathcal{L})$ of a Colding-Minicozzi lamination \mathcal{L} have class $C^{1,1}$ and are orthogonal to the leaves of \mathcal{L} . The proof by Meeks of the $C^{1,1}$ -regularity of $S(\mathcal{L})$ leads naturally to a unique related lamination metric on the minimal foliation on \mathcal{L} of N ([6]). This regularity theorem and lamination metric theorem have useful applications which include the classification of properly embedded minimal surfaces of finite genus in \mathbb{R}^3 and in other three-manifolds (see [9, 10, 8, 7, 11, 12]).

In all previously considered examples of sequences of locally simply connected minimal surfaces which converge to a minimal foliation \mathcal{L} with nonempty singular set of C^1 -convergence $S(\mathcal{L})$, the set $S(\mathcal{L})$ consisted of geodesics. While the first author had thought that this property might hold in general, it was pointed out to him by Frank Morgan that it was reasonable to expect that there exist compact embedded minimal annuli A_n that would converge to a Colding-Minicozzi limit minimal lamination $\tilde{\mathcal{L}}$ of an open set of \mathbb{R}^3 and with $S(\tilde{\mathcal{L}})$ being the unit circle in the (x_1, x_2) -plane. In fact, the following main theorem shows that in the case of \mathbb{R}^3 , any $C^{1,1}$ -curve $S(\mathcal{L})$ occurs as a singular set of C^1 -convergence of a Colding-Minicozzi limit minimal lamination.

Theorem 1 *Every properly embedded $C^{1,1}$ -curve α in an open set O in \mathbb{R}^3 has a neighborhood foliated by a particular Colding-Minicozzi limit minimal lamination \mathcal{L} with singular set of C^1 -convergence being α . The minimal leaves of this lamination \mathcal{L} are a $C^{1,1}$ -family of pairwise disjoint flat disks of varying radii. The disks are centered along and orthogonal to α . More generally, if N is a closed regular neighborhood of α formed by disjoint flat disks orthogonal to α and N' is a similarly defined foliation in the interior of N , then N' is contained in a Colding-Minicozzi minimal lamination which lies in N .*

The main step in the proof of Theorem 1 is to first prove the theorem when α is analytic with a compact exhaustion $\alpha(1) \subset \alpha(2) \subset \dots \subset \alpha(n) \subset \dots$, where $\alpha(i)$ is a

compact connected arc in α . We do this by giving an essentially explicit construction of a sequence of embedded compact *bent helicoids* $H_{\alpha,n}$ which contain $\alpha(n) \subset \alpha$ as an “axis” and whose Gauss maps rotate faster and faster along $\alpha(n)$ as $n \rightarrow \infty$. In this case, the $H_{\alpha,n}$ converge to a family of pairwise disjoint flat disks of varying radii orthogonal to α . The construction of the $H_{\alpha,n}$ is based on the classical Björling formula. Our main difficulty in proving Theorem 1 in the analytic case is to demonstrate the embeddedness of the $H_{\alpha,n}$ in a *fixed* neighborhood of $\alpha(n)$. The general case of the theorem follows from the analytic case by approximating α by a sequence of embedded analytic curves with uniformly locally bounded curvature, which is always possible for $C^{1,1}$ -curves.

In the special case that α is the unit circle in the (x_1, x_2) -plane, then, for all $n \in \mathbb{N}$, we can choose $\alpha(n) = \alpha$ and each compact annular bent helicoid $\overline{H}_n = H_{\alpha,n}$ contains α and is the image of a compact portion of a globally defined explicit periodic complete minimal immersion $f_n: \mathbb{C} \rightarrow \mathbb{R}^3$. In this case, we let H_n denote the image complete minimal annulus $f_n(\mathbb{C})$ and define compact embedded annuli $\overline{H}_n \subset H_n$ which converge to the limit minimal foliation \mathcal{L} of $\mathbb{R}^3 - x_3$ -axis by vertical half planes and with $S(\mathcal{L}) = \alpha$. We refer the reader to Section 3 for the analytic description of the parametrizations f_n of these special bent helicoids whose coordinate functions are expressed in terms of real and imaginary parts of the functions $\cos(z)$ and $\sin(z)$ for $z \in \mathbb{C}$. We also describe the analytic Weierstrass data for their image finite total curvature annuli H_n in terms of simple rational functions on the punctured complex plane $\mathbb{C} - \{0\}$.

The complete minimal annulus H_n has finite total curvature $-4\pi(n + 1)$ with the dihedral group $D(2n)$ of symmetries and contains n lines in the (x_1, x_2) -plane passing through the origin. The large symmetry group and the explicit representation of H_n allows us to define the compact *embedded* annuli $\overline{H}_n \subset H_n$ which converge to the minimal foliation \mathcal{L} of \mathbb{R}^3 . By way of approximation, this special case of a circle plays a key role in the proof of Theorem 1 in the more general case where α is an arbitrary properly embedded analytic curve in an open set O . This is because at every point of the analytic curve the related bent helicoids that we construct are closely approximated by the related bent helicoids of the second order approximately osculating circle at the point. Based on our construction of these bent helicoids and the $C^{1,1}$ -regularity theorem of Meeks [6, 5], we ask the following related question.

Question 1 *Is there a natural generalization of Theorem 1 to Riemannian three-manifolds?*

It turns out that the bent helicoids H_n also make sense for values $n = k - \frac{1}{2}$, where $k \in \mathbb{N}$, and for these fractional values the image surface is a complete immersed minimal Möbius strip. One special case of these bent helicoids was known before, namely $n = \frac{1}{2}$. This example is the Meeks’ Minimal Möbius strip of finite total curvature -6π defined in [4], see Figure 1.

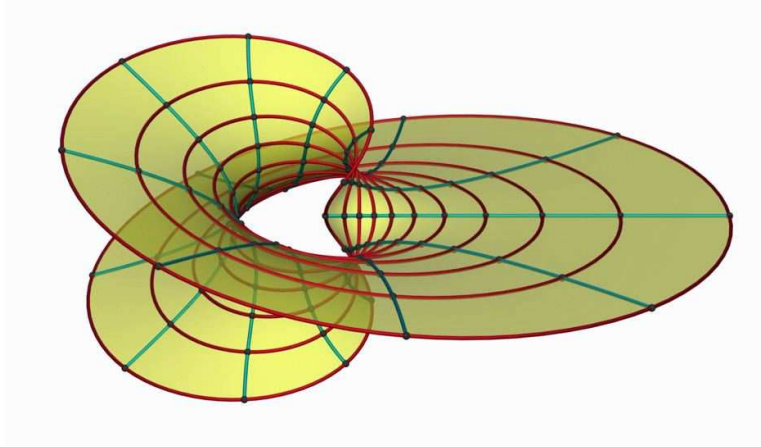


Figure 1: The complete minimal Möbius strip

For larger integer values n , near the unit circle the surface H_n looks like a bent helicoid:

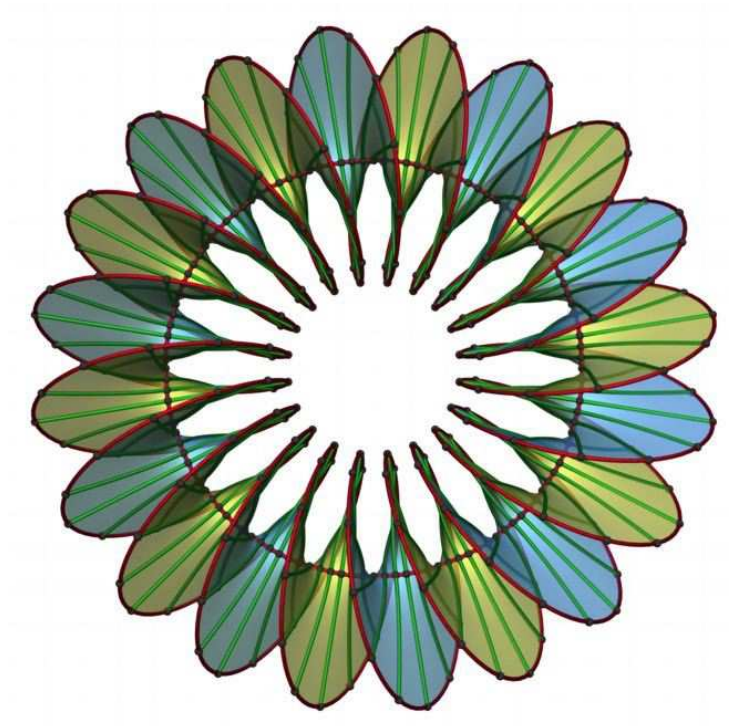


Figure 2: The bent helicoid for $n=10$

We would like to thank Bruce Solomon for helpful conversations about regularity questions.

2 Björling's theorem and the analytic representation of bent helicoids in the circular case.

We now recall Björling's theorem [2]. Let $c: [a, b] \rightarrow \mathbb{R}^3$ be any real analytic curve and $n: [a, b] \rightarrow \mathbb{S}^2 \subset \mathbb{R}^3$ be any real analytic vector field perpendicular to $c'(t)$. Consider $[a, b] \times \{0\} \subset \mathbb{C}$. By analyticity, there are a small positive ε and unique holomorphic extensions $c: [a, b] \times (-\varepsilon, \varepsilon) \rightarrow \mathbb{C}^3$, and $n: [a, b] \times (-\varepsilon, \varepsilon) \rightarrow \mathbb{C}^3$. Using these extensions, we define for $z = x + yi \in \mathbb{C}$

$$F(z) = \operatorname{Re} \left(c(z) - i \int_0^z n(w) \times c'(w) dw \right).$$

This is a minimal map that extends c and n in the sense that for $t \in [a, b]$, $F(t) = c(t)$ and $n(t)$ is the surface normal.

This formula was used by H.A. Schwarz to prove the classical reflection principles for minimal surfaces and to prove that the helicoid is the only ruled minimal surface besides the plane.

On the other hand, the above formula has not produced other globally interesting examples of minimal surfaces. This is mainly due to the fact that the Björling integral is usually impossible to evaluate explicitly, making it hard to say something about global properties of the minimal surfaces. In the case of the unit circle in the (x_1, x_2) -plane, there is a natural analytic parametrization as well as a natural sequence of analytic unit normal fields for which we can explicitly evaluate this integral to produce a sequence of Björling surfaces.

Let $c(t) = (\cos t, \sin t, 0)$ be the usual parametrization of the unit circle in the (x_1, x_2) -plane. A basis of normal fields along c is given by

$$\begin{aligned} n_1(t) &= -c(t), \\ n_2(t) &= (0, 0, 1). \end{aligned}$$

Define a new normal field with relative rotational speed $a \in \mathbb{R}^+$ by

$$n(t) = \cos(at)n_1(t) + \sin(at)n_2(t).$$

For $z \in \mathbb{C}$, we let $c(z), n(z)$ be the related vector valued holomorphic functions mapping \mathbb{C} to \mathbb{C}^3 . Then, using Björling's formula [2],

$$F(z) = \operatorname{Re} \left(c(z) - i \int_0^z n(w) \times c'(w) dw \right)$$

defines a minimal surface with parameter domain \mathbb{C} which extends the circle $c(t)$ and has $n(t)$ as the Gauss map along the circle. We refer to this surface as the *bent helicoid* H_a . Here we consider $c: \mathbb{R} \rightarrow \mathbb{R}^3$ to be a parametrized curve with related $n(t)$ along it; when $a \in \mathbb{N} \subset \mathbb{R}$, then $n(t)$ is well defined on the image circle $\mathbb{S}^1(1)$.

For a fixed value $a \in \mathbb{R}^+$, the conformal harmonic map $F: \mathbb{C} \rightarrow \mathbb{R}^3$ is explicitly calculated to be:

$$F(z) = \operatorname{Re} \int_0^z \begin{pmatrix} i \cos(w) \sin(aw) - \sin(w) \\ \cos(w) + i \sin(w) \sin(aw) \\ i \cos(aw) \end{pmatrix} dw$$

$$\stackrel{a \neq 1}{=} \operatorname{Re} \begin{pmatrix} \cos(z) - \frac{i(\cos(z) \cos(az)a - a + \sin(z) \sin(az))}{a^2 - 1} \\ \sin(z) - \frac{i(a \cos(az) \sin(z) - \cos(z) \sin(az))}{a^2 - 1} \\ \frac{i \sin(az)}{a} \end{pmatrix}.$$

Moreover, one can now convert this data for H_a to data for the classical Weierstrass representation

$$F(z) = \frac{1}{2} \int^z \left(\frac{1}{G} - G, i \left(\frac{1}{G} + G \right), 2 \right) \cdot dh.$$

This conversion produces a stereographically projected Gauss map

$$G(z) = -e^{iz} \frac{\cos(az)}{1 - \sin(az)}$$

and a complexified height differential

$$dh = i \cos(az) dz.$$

After the substitution $w = e^{iz}$, and for $a = n \in \mathbb{N}$, then

$$G(w) = -w \frac{w^n + i}{iw^n + 1},$$

$$dh = \frac{1}{2w} (w^n + w^{-n}) dw.$$

Thus, in this case, we see that $H_a = H_n$ is a complete minimal surface of a finite total curvature $-4\pi(n+1)$ and with parameter domain $\mathbb{C} - \{0\}$.

For $n = 0$, we recover the familiar Weierstrass representation of the catenoid.

3 The geometry and embeddedness of fundamental pieces of bent helicoids in the circular case

We now collect some simple properties of the bent helicoids H_a :

- Proposition 1**
1. For $a \in \mathbb{N}$, the immersion $F(z): \mathbb{C} \rightarrow \mathbb{R}^3$ is 2π periodic in the sense that $F(z) = F(z + 2\pi)$.
 2. The vertical coordinate lines $x = t_k = \frac{2k+1}{2a}\pi$ are mapped to the straight lines $s \mapsto s(\cos(t_k), \sin(t_k), 0)$
 3. The 180 degree rotations around the points $t_k = \frac{k}{a}\pi$ in the domain \mathbb{C} induce isometries of the surface which are 180 degree rotations about the lines $s \mapsto s(\cos(t_k), \sin(t_k), 0)$ (orthogonal to the surface) in \mathbb{R}^3 .
 4. The surface is invariant under rotation by angle $\frac{\pi}{a}$ about the x_3 -axis.

Proof: The first claim is trivial. We compute $f(t_k + ti)$ to be

$$\frac{(-1)^k \cosh(at) \sinh(t) + \cosh(t) (a^2 - (-1)^k \sinh(at)a - 1)}{a^2 - 1} (\cos(t_k), \sin(t_k), 0),$$

which proves the second claim. Alternatively, one can also see this from the uniqueness of the Björling solution as follows. At the points $t_k = \frac{2k+1}{2a}\pi$, we have

$$\begin{aligned} c(t_k) &= (\cos(t_k), \sin(t_k), 0), \\ n(t_k) &= (0, 0, (-1)^k). \end{aligned}$$

Since a rotation around the line $s \mapsto s(\cos(t_k), \sin(t_k), 0)$ maps the Björling data c and n to c and $-n$, it must map the surface $H(a)$ to the same surface with reversed orientation (by the uniqueness of the Björling solution). Because the line is tangent to the surface at $c(t_k)$, it must lie entirely on the surface.

The remaining claims are proven in a similar fashion. □

Proposition 2 *The conformal factor of the metric of $H(a)$ with conformal parametrization $F(x, y) = F(x + yi): \mathbb{C} \rightarrow \mathbb{R}^3$ is*

$$\lambda(x, y) = |F_x| = |F_y| = \cosh(y) \cosh(ay) - \sin(ax) \sinh(y)$$

and the tangent vector of the curve $y \mapsto F(0, y)$ is

$$F_y(0, y) = (\sinh(y), \sinh(y) \sinh(ay), -\cosh(ay)).$$

Proof: By direct computation. □

Moreover, the simple form of the Weierstrass data allows us to establish some other remarkable properties of this family of surfaces, which we now describe.

The following lemma shows that the image of the vertical half-lines $T \mapsto x \pm Ti$ are (for large T) close to horizontal half-lines in space.

Lemma 1

$$\lim_{T \rightarrow \infty} e^{-(a+1)T} F(x + Ti) = \frac{1}{4(a+1)} (-\sin((a+1)x), \cos((a+1)x), 0),$$

$$\lim_{T \rightarrow -\infty} e^{(a+1)T} F(x + Ti) = \frac{1}{4(a-1)} (\sin((a+1)x), -\cos((a+1)x), 0).$$

Proof: This follows from the integrated formula of F by straightforward computation. \square

Corollary 1 For $a > 2$, the image under F of $[-\frac{\pi}{2a}, \frac{\pi}{2a}] \times (-\infty, \infty)$ is embedded, except at the origin in \mathbb{R}^3 where the two boundary lines intersect. Hence, the image under F of the fundamental piece $(-\frac{\pi}{2a}, \frac{\pi}{2a}) \times (-\infty, \infty)$ is an embedded surface.

Proof: Subdivide for any $T > 0$ the domain $[-\frac{\pi}{2a}, \frac{\pi}{2a}] \times (-T, T)$ into two closed pieces R_T^\pm depending on the sign of y . The boundary of $F(R_T^+)$ consists of four pieces: the circular arc $\alpha_1 = \alpha([-\frac{\pi}{2a}, \frac{\pi}{2a}])$, the rays $\alpha_2 = F(\{-\frac{\pi}{2a}\} \times [0, T])$ and $\alpha_3 = F(\{\frac{\pi}{2a}\} \times [0, T])$ and the image arc $\alpha_4 = F([-\frac{\pi}{2a}, \frac{\pi}{2a}] \times \{T\})$.

For large T , the total curvature of the boundary of $F(R_T^+)$ is asymptotically $\frac{2\pi}{a} + 3\pi < 4\pi$ when $a > 2$. In addition, this boundary is embedded, because the respective arcs are disjoint and embedded as individuals. Thus the entire image $F(R_T^+)$ is embedded (for $a > 2$) by [3] for any large T , and thus also $F(R_\infty^+)$.

As the third coordinate function $\frac{1}{a} \cos(ax) \sinh(ay)$ changes sign with y , $F(R_\infty^+)$ is contained in the closed upper half space and intersects the x_1x_2 -plane only in the two rays α_2 and α_3 . The 180° rotation about the x_1 -axis rotates $F(R_\infty^+)$ into $F(R_\infty^-)$. Hence the whole surface is embedded except at the origin as the intersection point of the two lines. This proves the corollary. \square

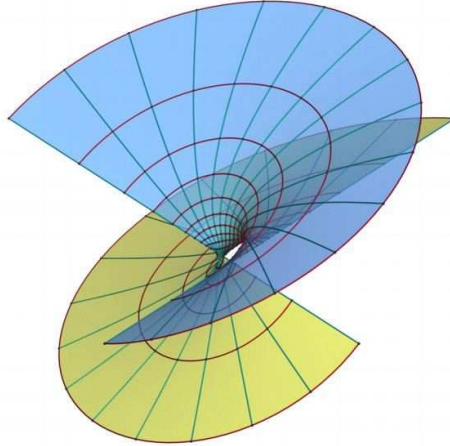


Figure 3: An embedded fundamental piece of H_a for $a = 2$.

4 Approximation results

This section has two goals. First, in the circle case, we give an explicit estimate for how close the y -curves $y \mapsto F(x, y)$ are to the lines L_x in \mathbb{R}^3 passing through $F(x, 0)$ and tangent to the curve at this point. This estimate shows that on compact subsets of \mathbb{R}^3 , as $a \rightarrow \infty$, the y -curves converge C^k to the corresponding line in $\{L_x\}_{x \in \mathbb{R}}$, and so, on a given large compact set of \mathbb{R}^3 and for $a \in \mathbb{N}$ sufficiently large, H_a closely approximates the related ruled surface along the circle. However, our estimates are not sufficient to prove Theorem 1 by comparison with the ruled surface; we get around this problem in the next section by using the large symmetry group of H_n . Second, for an analytic curve α , we compare a general bent helicoid $H_{\alpha, n}$ (to be defined) to the circular helicoid \bar{H}_a in terms of how far the surfaces are apart along the related y -curve lines that begin near a point $\alpha(x)$, when the circle is the second order approximation to α at $\alpha(x)$.

For the first part, we compare the minimal surface H_a with a suitably parameterized ruled surface

$$R(x, y) = c(x) + t_a(y)c'(x) \times n(x),$$

where

$$\begin{aligned} t_a(y) &= \frac{a \cosh(y) \sinh(ay) - \cosh(ay) \sinh(y)}{a^2 - 1} - \sin(ax)(\cosh(y) - 1) \\ &\approx \frac{\cosh(y) \sinh(ay)}{a} \quad \text{for } a \text{ large} \end{aligned}$$

is the primitive of $|F_y(x, y)|$.

This ruled surface has the same core circle as F and its ruling lines point in the same direction as the tangent vectors $F_y(x, 0)$. The ruling lines are parameterized so that their speed is equal to the speed $|F_y(x, y)|$ given by Proposition 2. While the ruled surface R is a poor approximation for F when $y = \text{Im } z$ is large (by Lemma 1), it becomes better and better in the range $|y| < d = d(a)$, where d is determined so that the curves $F(x \pm di)$ stays at distance 1 away from the core circle by using the approximate expression for $t_a(y)$ to solve $t_a(d) = 1$ for d . This motivates (for a large) our definition of d :

$$d = d(a) = \frac{\log(a)}{a}.$$

Observe that

$$|R(x, d) - R(x, 0)| \approx 1 \approx |R(x, -d) - R(x, 0)|.$$

This means that the curves $\text{Im } z = \pm d$ are approximately mapped onto the boundary of the tube of radius 1 around the unit circle.

Observe also that for $x = t_k = \frac{k}{a}\pi$, the parameterizations $F(t_k, y)$ and $R(t_k, y)$ coincide. Now we can state and prove our approximation theorem.

Lemma 2 For $|y| \leq d(a)$, we have

$$|R(x, y) - F(x, y)| \leq d(a) \quad \text{and } d(a) \rightarrow 0 \text{ as } a \rightarrow \infty.$$

Proof: By the definitions, we have

$$\frac{\partial}{\partial y} (R(x, y) - F(x, y)) = \begin{pmatrix} \cos(ax) \sinh(y) (\sin(x) \sinh(ay) - \cos(x) \cos(ax)) \\ -\cos(ax) \sinh(y) (\cos(ax) \sin(x) + \cos(x) \sinh(ay)) \\ -\cos(ax) ((\cosh(y) - 1) \cosh(ay) - \sin(ax) \sinh(y)) \end{pmatrix}.$$

By direct computation, we obtain

$$\left| \frac{\partial}{\partial y} (R(x, y) - F(x, y)) \right|^2 = 4 \cos^2(ax) \cosh(ay) \sinh^2\left(\frac{y}{2}\right) (\cosh(y) \cosh(ay) - \sin(ax) \sinh(y)).$$

From these formulas, it follows that for $|y| < d$, then

$$\left| \frac{\partial}{\partial y} (R(x, y) - F(x, y)) \right| \leq \cosh(ay) |\sinh(y)|,$$

and so,

$$\begin{aligned} |R(x, y) - F(x, y)| &\leq \int_0^d \cosh(ay) |\sinh(y)| dy \\ &\leq \frac{-\cosh(d) \cosh(ad) + a \sinh(d) \sinh(ad) + 1}{a^2 - 1} \\ &\leq d, \end{aligned}$$

as claimed. □

Our next goal is to compare the Björling surfaces associated to arbitrary analytic curves and normal frames.

Let $\tilde{c}(t)$ be an analytic curve with analytic normal frame $\tilde{c}'(t), \tilde{n}_1(t), \tilde{n}_2(t)$. Assume that $|c(t) - \tilde{c}(t)| \leq Ct^2$ and $|n_j(t) - \tilde{n}_j(t)| \leq Ct^2$ for $t \in (-\epsilon, \epsilon)$ and $j = 1, 2$. Here we think of $c(t)$ as being an osculating circle for $\tilde{c}(t)$ at $\tilde{c}(0)$, but our argument below works for any curves that are close to second order.

We assume that both c and \tilde{c} are parameterized by arc length. Introduce the spinning normal fields for \tilde{c}

$$\tilde{n}(t) = \cos(at) \tilde{n}_1(t) + \sin(at) \tilde{n}_2(t).$$

Define the Björling surfaces

$$\tilde{F}(z) = \operatorname{Re} \left(\tilde{c}(z) - i \int_0^z \tilde{n}(w) \times \tilde{c}'(w) dw \right).$$

As $c' \times n_1 = n_2$, we have

$$c' \times n = \cos(at)n_2(t) - \sin(at)n_1(t)$$

(and similarly for \tilde{c}).

This allows us to estimate the distance between the parameterizations $F(z)$ and $\tilde{F}(z)$.

Lemma 3 For $|\operatorname{Im} z| \leq d = \frac{\log(a)}{a}$ and $|\operatorname{Re} z| < \frac{\pi}{a}$ and sufficiently large a

$$|\tilde{F}(z) - F(z)| \leq 6C \frac{(\log a)^2}{a^2}$$

Proof: The idea is to integrate by parts twice.

$$\begin{aligned} |\tilde{F}(z) - F(z)| &\leq \left| \tilde{c}(z) - c(z) - i \int_0^z \cos(aw)(\tilde{n}_2(w) - n_2(w)) - \sin(aw)(\tilde{n}_1(w) - n_1(w)) dw \right| \\ &= C|z|^2 + \left| \frac{\sin(aw)}{a}(\tilde{n}_2(w) - n_2(w)) - \frac{\cos(aw)}{a}(\tilde{n}_1(w) - n_1(w)) \right|_{w=0}^z + \\ &\quad + \left| \int_0^z \frac{\sin(aw)}{a}(\tilde{n}'_2(w) - n'_2(w)) - \frac{\cos(aw)}{a}(\tilde{n}'_1(w) - n'_1(w)) dw \right| \\ &\leq C|z|^2(1 + \left| \frac{\sin(aw)}{a} \right| + \left| \frac{\cos(aw)}{a} \right|) + C|z|(\left| \frac{\sin(aw)}{a^2} \right| + \left| \frac{\cos(aw)}{a^2} \right|) + \\ &\quad + \left| \int_0^z \frac{\cos(aw)}{a^2}(\tilde{n}''_2(w) - n''_2(w)) - \frac{\sin(aw)}{a^2}(\tilde{n}''_1(w) - n''_1(w)) dw \right| \\ &\leq C|z|^2(1 + \left| \frac{\sin(aw)}{a} \right| + \left| \frac{\cos(aw)}{a} \right|) + 2C|z|(\left| \frac{\sin(aw)}{a^2} \right| + \left| \frac{\cos(aw)}{a^2} \right|). \end{aligned}$$

Now we use that the domain is $|\operatorname{Im} z| \leq d = \frac{\log(a)}{a} \approx \frac{\sinh^{-1}(a)}{a}$ and $|\operatorname{Re} z| < \frac{\pi}{a} < \frac{\log(a)}{a}$, so that for a large, $|z| < \sqrt{2}d$. In this domain, we get

$$|\tilde{F}(z) - F(z)| \leq 6Cd^2 + 2C\frac{d}{a}.$$

As $d = \frac{\log(a)}{a}$,

$$|\tilde{F}(z) - F(z)| \leq 6C \frac{(\log a)^2}{a^2}.$$

□

5 The proof of Theorem 1 in the circular case.

In this section, we prove the following version of Theorem 1 in the circular case.

Let T_R be the $(R - \frac{1}{R})$ -neighborhood in \mathbb{R}^3 of the circle $\mathbb{S}^1(R) = \{x_1^2 + x_2^2 = R^2\} \subset \mathbb{R}^2 \times \{0\}$. This domain is the region within which we want to consider embeddedness first.

Theorem 2 *For each $a \in \mathbb{N}$ and $R > 1$, let $\widehat{H}_{a,R}$ be the component of the embedded minimal disk $F([\frac{-\pi}{2a}, \frac{\pi}{2a}] \times \mathbb{R}) \cap T_R$ containing the circular arc $F([\frac{-\pi}{2a}, \frac{\pi}{2a}] \times \{0\})$. For $a \in \mathbb{N}$ sufficiently large, the orbit $H_{a,R}$ of $\widehat{H}_{a,R}$ under the cyclic group \mathbb{Z}_{2a} generated by rotation around the positive x_3 -axis by the angle $\frac{\pi}{a}$, is an embedded minimal annulus. Furthermore, as $a \rightarrow \infty$ and R is fixed, the annuli $H_{a,R}$ converge to the minimal foliation \mathcal{L}_R of T_R consisting of the flat disks of radii $R - \frac{1}{R}$ centered at points of $\mathbb{S}^1(R)$ and orthogonal to $\mathbb{S}^1(R)$ and with $S(\mathcal{L}_R) = \mathbb{S}^1(R)$. In particular, there exists a divergent sequence of $R_n \rightarrow \infty$ as $n \rightarrow \infty$, so that the bent helicoids $\overline{H}_n = H_{n,R_n}$ are embedded and converge to the Colding-Minicozzi limit minimal lamination \mathcal{L} of $\mathbb{R}^3 - x_3$ -axis consisting of leaves which are half planes with axis the x_3 -axis and with $S(\mathcal{L}) = \mathbb{S}^1(1)$.*

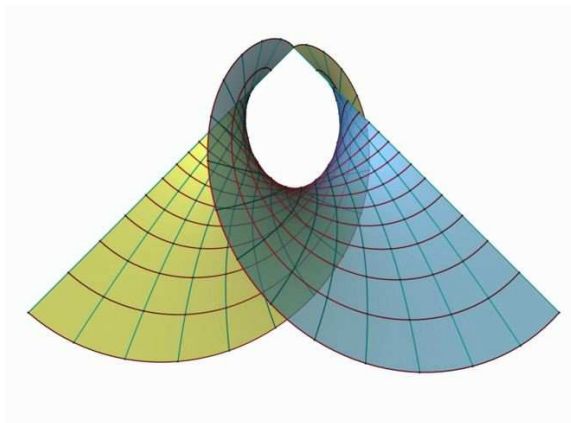


Figure 4: A fundamental piece of H_a in a “sector” for $a = 2$.

Proof: Fix $R > 1$ and $a \in \mathbb{N}$. In Corollary 1 in section 3, we proved that the $\widehat{H}_a = F([\frac{-\pi}{2a}, \frac{\pi}{2a}] \times (-\infty, \infty))$ is a fundamental piece of the surface H_a , which is embedded in \mathbb{R}^3 with boundary two straight lines. We now denote these two lines by $L(\frac{-\pi}{2a}), L(\frac{\pi}{2a})$ and remark that they lie in the (x_1, x_2) -plane and make an angle of $\frac{\pi}{a}$ at the origin. Let $H_{a,R}$ denote the immersed minimal surface component of $H_a \cap T_R$ that contains $\mathbb{S}^1(1)$. Note that $H_{a,R}$ is the \mathbb{Z}_{2a} -orbit of the embedded component $\widehat{H}_{a,R}$ of $\widehat{H}_a \cap T_R$ that contains the circular arc $\sigma_a = F([\frac{-\pi}{2a}, \frac{\pi}{2a}] \times \{0\})$, where \mathbb{Z}_{2a} is generated by rotation by $\frac{\pi}{a}$ around

the x_3 -axis. More precisely, $H_{a,R}$ is the image under F of the component of $F^{-1}(T_R) \cap ([-\frac{\pi}{2a}, \frac{\pi}{2a}] \times (-\infty, \infty))$ that contains the interval $[-\frac{\pi}{2a}, \frac{\pi}{2a}] \times \{0\}$.

By the results in the previous section, for large values of $a \in \mathbb{N}$, the surface $\widehat{H}_{a,R}$ is a compact embedded disk which intersects ∂T_R almost orthogonally in two almost circular arcs in ∂T_R . These arcs join the end points of line segments $l(\frac{-\pi}{2a}) \subset L(\frac{-\pi}{2a}) \cap T_R$, $l(\frac{\pi}{2a}) \subset L(\frac{\pi}{2a}) \cap T_R$, which make up the remainder of $\partial \widehat{H}_{a,R}$. If the embedded disk $\widehat{H}_{a,R}$ were contained in the sector of \mathbb{R}^3 containing the circular arc σ_a and bounded by the vertical half planes containing $l(\frac{-\pi}{2a}), l(\frac{\pi}{2a})$, respectively, then the \mathbb{Z}_{2a} -orbit $H_{a,R}$ of $\widehat{H}_{a,R}$ would be an embedded annulus. Although $\widehat{H}_{a,R}$ fails to be contained in this sector (see Figure 4), we shall still be able to prove that $H_{a,R}$ is an embedded minimal annulus for $a \in \mathbb{N}$ large.

Consider T_R with the ‘‘cylindrical’’ coordinates (θ, x) with $x \in D_R$, where D_R is the disk in the (x_1, x_3) -plane of radius $R - \frac{1}{R}$ centered at the point $(R, 0, 0)$. For $a \in \mathbb{N}$ sufficiently large and for $\varepsilon(a) = \frac{1}{a}$, the sequence of $\varepsilon(a)$ -tubular neighborhoods $\mathbb{S}_{\varepsilon(a)}^1(1)$ of $\mathbb{S}^1(1)$ in T_R , when intersected with $H_{a,R}$ and then translated by $(-1, 0, 0)$ and expanded homothetically by the factor a , produces a sequence of minimal annuli which converges on compact subsets of \mathbb{R}^3 to a helicoid intersected with the solid cylinder of radius 1 around the x_2 -axis (this follows by direct calculation). For $x \in D_R$, let C_x denote the horizontal circle $\{(\theta, x) \mid 0 \leq \theta < 2\pi\}$ in our cylindrical coordinates of T_R in $\mathbb{R}^3 - x_3$ -axis. It follows that for $a \in \mathbb{N}$ large, $\widehat{H}_{a,R}$ intersects every horizontal circle $C_x \subset \mathbb{S}_{\varepsilon(a)}^1(1) - \mathbb{S}^1(1)$, transversely in a single point. Furthermore, for a large, every horizontal circle $C_x \subset (T_R - \mathbb{S}_{\varepsilon(a)}^1(1))$, intersects $\widehat{H}_{a,R}$ transversely in a single point and the angle of intersection is uniformly bounded away from zero by a positive constant which is independent of a (this follows from our formula for the Gauss map of $\widehat{H}_{a,R}$ and the estimates in the previous section). Since every such circle $C_x \subset (T_R - \mathbb{S}^1(1))$ is invariant under \mathbb{Z}_{2a} , it follows that for $a \in \mathbb{N}$ sufficiently large, $H_{a,R}$ is an embedded minimal annulus.

In cylindrical coordinates, we see that for $a \in \mathbb{N}$ sufficiently large, $H_{a,R} - \mathbb{S}^1(1)$ is a two component multigraph over $D_R - \{(1, 0, 0)\}$ invariant under the action of \mathbb{Z}_{2a} . Also note that each of these multigraphs is stable with a positive Jacobi function induced by the killing field of \mathbb{R}^3 generated by rotation around the x_3 -axis. In particular, by curvature estimates for stable minimal surfaces [14], we see that the sequence of surfaces $\{H_{a,R}\}_{a \in \mathbb{N}}$ has uniformly locally bounded curvature in any ball in T_R of positive distance from $\mathbb{S}^1(1)$.

It is now standard (e.g. see the proof of Theorem 1.6 in [13]) that a subsequence of the surfaces $\{H_{a,R} - \mathbb{S}^1(1)\}_{a \in \mathbb{N}}$ converges C^2 to a minimal lamination $\widehat{\mathcal{L}}_R$ of $T_R - \mathbb{S}^1(1)$ whose leaves are mapped to other leaves under any rotation around the x_3 -axis. Clearly, the leaves of $\widehat{\mathcal{L}}_R$ are punctured flat disks of radius $R - \frac{1}{R}$ which are orthogonal to $\mathbb{S}^1(1)$ and are centered along $\mathbb{S}^1(R)$ (for example, consider the values of the Gauss map of $H_{a,R}$ away from $\mathbb{S}^1(1)$ for $a \in \mathbb{N}$ large). Thus, $\widehat{\mathcal{L}}_R$ extends to the foliation \mathcal{L}_R of T_R by flat disks orthogonal to $\mathbb{S}^1(1)$. Since the tangent planes of the $H_{a,R}$ are orthogonal to the tangent

planes to \mathcal{L}_R along $\mathbb{S}^1(1)$, the sequence $\{H_{a,R}\}_{a \in \mathbb{N}}$ converges to \mathcal{L}_R with singular set of C^1 -convergence $S(\mathcal{L}_R) = \mathbb{S}^1(1)$. This concludes the proof of the first statement of the theorem. The second statement then follows by applying a standard diagonal argument. \square

6 The proof of Theorem 1 in the analytic case.

In the last section, we proved Theorem 1 in the case the curve α is the unit circle in the (x_1, x_2) -plane and our open set is \mathbb{R}^3 . We now prove the theorem in the special case where α is a properly embedded analytic curve in an open set O .

In what follows, it suffices to consider α an open curve. If the curve is closed, one faces the additional technical complication that the normal fields need to close up. Without loss of generality, we may assume that our analytic curve $\alpha(t)$ has unit speed with analytic frame $\alpha'(t), n_1(t), n_2(t) = \alpha'(t) \times n_1(t)$. Let

$$n(t) = \cos(at)n_1(t) + \sin(at)n_2(t).$$

For $a \in \mathbb{R}^+$, let $H_{\alpha,a}$ be related Björling surface or *bent helicoid*. Fix a point $p \in \alpha(t)$, which we may assume has the form $p = \alpha(0)$. After a rigid motion, we may assume that

$$\alpha'(0) = (1, 0, 0), \quad \langle \alpha''(0), (-1, 0, 0) \rangle = \kappa \geq 0.$$

If the curvature $\kappa \neq 0$, then, after a dilation, we also may assume that $\kappa = 1$.

The analysis of the case $\kappa = 0$ and the case $\kappa = 1$ are similar. We only consider the case $\kappa \neq 0$; in both cases, one compares the geometry of $H_{\alpha,a}$ with the geometry of a standard surface where the standard surface is a helicoid if $\kappa = 0$ or the bent helicoid H_a when $\kappa = 1$. So, assume now that $\kappa = 1$.

Consider a continuous family \mathcal{D} of pairwise disjoint disks D_t which are orthogonal to $\alpha(t)$ for each t and which lie in the interior of another such family $\tilde{\mathcal{D}}$. Note that for $R > 1$ fixed and large, there exists a small $\varepsilon > 0$ such that the family of disks D_t , $-\frac{\varepsilon}{2} \leq t \leq \frac{\varepsilon}{2}$, are embedded and contained in the domain $T_R(\varepsilon) = \{(\theta, x) \in T_R \mid -\varepsilon \leq \theta \leq \varepsilon\}$, where T_R is defined just before the statement of Theorem 2 and the cylindrical coordinates on T_R are those introduced in the proof of Theorem 2. Theorem 1 in the case α is analytic easily follows from the following assertion, after restricting neighborhoods appropriately.

Assertion 1 *Fix $R > 1$. Then there exists a small $\varepsilon > 0$ such that for $a \in \mathbb{N}$ sufficiently large, the component $H_{\alpha,a}(\varepsilon)$ of $F_a([-\varepsilon, \varepsilon] \times (-\delta(\varepsilon), \delta(\varepsilon))) \cap T_R(2\varepsilon)$ containing $\alpha_\varepsilon = F_a([-\varepsilon, \varepsilon] \times \{0\})$ is an embedded disk. Here, the domain $[-\varepsilon, \varepsilon] \times (-\delta(\varepsilon), \delta(\varepsilon))$ is a box neighborhood of $[-\varepsilon, \varepsilon] \times \{0\} \subset \mathbb{C}$, where the Björling data is defined.*

Proof: We first consider the special case where $n_1(0) = (-1, 0, 0)$. Let $\tilde{\alpha}(t) = (\cos(t), \sin(t), 0)$ and $\tilde{n}_1(t) = -\tilde{\alpha}(t)$, $\tilde{n}_2(t) = (0, 0, 1)$. The data for α and $\tilde{\alpha}$ agree to second order at $t = 0$ and the data for $\tilde{\alpha}$ produces the Björling bent helicoids H_n for $n \in \mathbb{N}$. By the proof of Theorem 2, for $a \in \mathbb{N}$ large, the component $H_{\tilde{\alpha}, a}(\varepsilon)$ is an embedded disk.

As in the case α was the circle $\tilde{\alpha}$, which we considered in the previous section, for $a \in \mathbb{N}$ large, on the scale of curvature and for any sufficiently small $\varepsilon > 0$, the surface $H_{\alpha, a}(\varepsilon)$ is closely approximated near each point of α by homothetically shrunk helicoids initially contained in a cylinder of radius 1 around its axis, in the following sense. At every point $q \in \alpha_\varepsilon = \alpha([-\varepsilon, \varepsilon])$ and inside the $\frac{1}{a}$ -neighborhood $N_{\mathbb{R}^3}(\alpha_\varepsilon, \frac{1}{a})$ of α_ε in \mathbb{R}^3 the related sequence of surfaces under dilations by the factor a at q , converge to a helicoid with axis tangent to α at q . Note that $N_{\mathbb{R}^3}(\alpha_\varepsilon, \frac{1}{a}) \cap H_{\alpha, a}(\varepsilon) = N(\alpha_\varepsilon, \frac{1}{a})$ is a simply connected neighborhood of α_ε in $H_{\alpha, a}(\varepsilon)$. Using the fact that $H_{\alpha, a}(\varepsilon)$ is closely approximated by a ruled surface, shows that for $a \in \mathbb{N}$ sufficiently large, the self-intersection set of $H_{\alpha, a}(\varepsilon)$ is disjoint from the $\frac{1}{a}$ -neighborhood of α_ε .

Let $\eta = \frac{2\pi}{a}$. Our approximation results imply that for $a \in \mathbb{N}$ large that $H_{\alpha, a}(\eta) - N_{\mathbb{R}^3}(\alpha_\eta, \frac{1}{a})$ consist of two parametrized disks S_+, S_- that are multi-graphs over $H_{\tilde{\alpha}, a}(\eta) - N_{\mathbb{R}^3}(\alpha_\eta, \frac{1}{a})$ of norm on the order of $(\frac{\log(a)}{a})^2$ for a sufficiently large (this estimate also depends on R but since R is fixed it can be assumed to be uniform in a). On the other hand, for a large, the distance between successive sheets of the two spiraling multigraphs $\tilde{S}_+, \tilde{S}_- \subset (H_{\tilde{\alpha}, a}(\eta) - N_{\mathbb{R}^3}(\alpha_\eta, \frac{1}{a}))$ is bounded from below by $\frac{C'}{a}$, where C' is a positive constant depending only on R .

When choosing $a \in \mathbb{N}$ large, the sheets of \tilde{S}_+ separate the sheets of the multigraphs S_- from each other (similarly \tilde{S}_- separates the sheets S_+ from each other), then the sheets of S_+ and S_- do not intersect. Since S_+ can be expressed as a small graph over \tilde{S}_+ with gradient bounded uniformly for $a \in \mathbb{N}$ large. Hence, $H_{\alpha, a}(\varepsilon)$ is an embedded disk for some fixed small $\varepsilon > 0$.

This completes the proof of the assertion under the assumption that $n_1(0) = (-1, 0, 0)$. In the case, $n_1(0) \neq (-1, 0, 0)$, one compares the surface $H_{\alpha, a}(\varepsilon)$, for large $a \in \mathbb{N}$, with $\overline{H}_a(\theta)$ where $\overline{H}_a(\theta)$ is the bent helicoid \overline{H}_a rotated so that the normal fields satisfy:

$$n_1(a, \theta)(0) = n_1(0).$$

Then one proceeds as above. Thus, the general case follows from our special case where $n_1(0) = (-1, 0, 0)$. This completes the proof of the assertion. \square

7 The proof of Theorem 1 in the $C^{1,1}$ -case.

Consider now an arbitrary properly embedded $C^{1,1}$ -curve α in an open set O of \mathbb{R}^3 . We can just consider the case where α is noncompact because the compact case follows from

the same arguments. Consider $\alpha: (a, b) \rightarrow \mathbb{R}^3$ to be a unit speed $C^{1,1}$ -parametrization of the image curve α . Fix a compact exhaustion

$$[a_1, b_1] \subset \dots \subset [a_n, b_n] \subset \dots$$

of (a, b) . Recall that a $C^{1,1}$ -curve $\alpha(t)$ has locally bounded curvature function $\kappa(t)$ defined almost everywhere; in fact, $\alpha'(t)$ is absolutely continuous with a related locally bounded difference quotient function $\widehat{\kappa}(t)$. Since α is a $C^{1,1}$ -curve, there exists a sequence of embedded unit speed analytic curves $\beta_n: [a_n, b_n] \rightarrow \mathbb{R}^3$ which converge C^1 to α . The β_n can be chosen to have uniformly bounded curvature at most $\min \widehat{\kappa}|_{[a_k, b_k]}$ on any fixed $[a_k, b_k] \subset [a_n, b_n]$ for $n \geq k$. Their related curvature functions are uniformly bounded by $\widehat{\kappa}(t)$.

To see this, first convolve the $C^{1,1}$ -curve with a mollifier. This gives a C^∞ -curve which will be uniformly close to the original curve. The Lipschitz bound on the velocity then bounds the second derivative of the mollified curve. (Differentiate the convolution twice and integrate by parts once). Then, these C^∞ -curves can be approximated by analytic curves β_n converging to α and with curvature functions converging to $\widehat{\kappa}(t)$. It then follows from arguments of the previous section that for fixed n and k with $n > k$, there is a sequence of bent helicoids containing $\beta_n[a_k, b_k]$ which give rise to a Colding-Minicozzi minimal lamination of the $\lambda \widehat{\kappa}(t)$ -normal bundle of $\beta_n[a_k, b_k]$ for any positive $\lambda < 1$. A standard diagonal argument together with arguments from the analytic case then produces a sequence of bent helicoids that converges to a limit minimal lamination satisfying the requirements of Theorem 1.

William H. Meeks, III at bill@gang.umass.edu,
Math Department, University of Massachusetts, Amherst, MA 01003.

Matthias Weber matweber@indiana.edu,
Math Department, University of Indiana, Bloomington, IN 47405.

References

- [1] T. H. Colding and W. P. Minicozzi II. The space of embedded minimal surfaces of fixed genus in a 3-manifold IV; Locally simply-connected. *Annals of Math.*, 160:573–615, 2004.
- [2] U. Dierkes, S. Hildebrandt, A. Küster, and O. Wohlrab. *Minimal Surfaces I*. Grundlehren der mathematischen Wissenschaften 296. Springer-Verlag, 1992.
- [3] T. Ekholm, B. White, and D. Wienholtz. Embeddedness of minimal surfaces with total curvature at most 4π . *Annals of Math.*, 155:209–234, 2002.

- [4] W. H. Meeks III. The classification of complete minimal surfaces with total curvature greater than -8π . *Duke Math. J.*, 48:523–535, 1981.
- [5] W. H. Meeks III. The regularity of the singular set in the Colding and Minicozzi lamination theorem. *Duke Math. J.*, 123(2):329–334, 2004.
- [6] W. H. Meeks III. The lamination metric for a Colding-Minicozzi minimal lamination. *Illinois J. of Math.*, 49:645–658, 2005.
- [7] W. H. Meeks III, J. Pérez, and A. Ros. Embedded minimal surfaces: removable singularities, local pictures and parking garage structures, the dynamics of dilation invariant collections and the characterization of examples of quadratic curvature decay. Preprint.
- [8] W. H. Meeks III, J. Pérez, and A. Ros. The geometry of minimal surfaces of finite genus III; bounds on the topology and index of classical minimal surfaces. Preprint.
- [9] W. H. Meeks III, J. Pérez, and A. Ros. The geometry of minimal surfaces of finite genus I; curvature estimates and quasiperiodicity. *J. of Differential Geometry*, 66:1–45, 2004.
- [10] W. H. Meeks III, J. Pérez, and A. Ros. The geometry of minimal surfaces of finite genus II; nonexistence of one limit end examples. *Invent. Math.*, 158:323–341, 2004.
- [11] W. H. Meeks III and H. Rosenberg. The minimal lamination closure theorem. *Duke Math. J.* (to appear).
- [12] W. H. Meeks III and H. Rosenberg. The theory of minimal surfaces in $M \times \mathbb{R}$. *Comment. Math. Helv.* (to appear).
- [13] W. H. Meeks III and H. Rosenberg. The uniqueness of the helicoid and the asymptotic geometry of properly embedded minimal surfaces with finite topology. *Annals of Math.*, 161:727–758, 2005.
- [14] R. Schoen. *Estimates for Stable Minimal Surfaces in Three Dimensional Manifolds*, volume 103 of *Annals of Math. Studies*. Princeton University Press, 1983. MR0795231, Zbl 532.53042.